On the Non-locality of the Electron-Photon Self-Energy: Application to Carbon Nanotube Photo-Detectors

M. Pourfath, O. Baumgartner, and H. Kosina
Institute for Microelectronics, TU Wien, 1040 Vienna, Austria
Email: {pourfath|baumgartner|kosina}@iue.tuwien.ac.at

***Abstract*—Carbon nanotubes have been considered in recent years for future opto-electronic applications because of their direct band-gap and the tunability of the band-gap with the tube diameter. The numerical challenges for the analysis of carbon nanotube based photo-detectors are studied. The results indicate the non-locality of electron-photon interaction. For accurate analysis it is essential to include many off-diagonals of the electron-photon self-energy.**

I. Introduction

Carbon nanotubes (CNTs) have been extensively studied in recent years due to their exceptional electronic, opto-electronic, and mechanical properties [1]. Owing to excellent optical properties of CNTs, an all-CNT electronic and opto-electronic circuit can be envisioned. The direct band-gap and its tunability with the CNT diameter renders them as suitable candidates for opto-electronic devices, especially for infra-red (IR) applications [2, 3] due to the relatively narrow band gap.

IR photo detectors based on carbon nanotube field effect transistors (CNT-FETs) have been reported in [3–5]. To explore the physics of such devices self-consistent quantum mechanical simulations have been performed, employing the non-equilibrium Green's function formalism (NEGF). This method has been successfully utilized to investigate the characteristics of CNT-FETs [6–9]. We employed the NEGF method based on the tight-binding π-bond model to study quantum transport in IR photo detectors based on CNT-FETs.

II. Non-equilibrium Green's Function Formalism

The NEGF formalism initiated by Schwinger, Kadanoff, and Baym allows to study the time evolution of a many-particle quantum system. Knowing the single-particle Green's functions of a given system, one may evaluate single-particle quantities such as carrier density and current. The many-particle information about the system is cast into self-energies, which are part of the equations of motion for the Green's functions. Green's functions enable a powerful technique to evaluate the properties of a many-body system both in thermodynamic equilibrium and non-equilibrium situations [10].

Four types of Green's functions are defined as the non-equilibrium statistical ensemble averages of the single particle correlation operator. The greater Green's function $G^{>}$ and the lesser Green's function $G^{<}$ deal with the statistics of carriers. The retarded Green's function G^{R} and the advanced Green's function G^{A} describe the dynamics of carriers.

Under steady-state condition the equation of motion for the Green's functions can be written as [10]:

$$[E - H_0]\, G^{\mathrm{R,A}}(1,2) - \int d3\ \Sigma^{\mathrm{R,A}}(1,3) G^{\mathrm{r,a}}(3,2) = \delta_{1,2} \tag{1}$$

$$G^{\lessgtr}(1,2) = \int d3 \int d4\ G^{\mathrm{R}}(1,3) \Sigma^{\lessgtr}(3,4) G^{\mathrm{A}}(4,2) \tag{2}$$

The abbreviation $1 \equiv (\mathbf{r_1}, t_1)$ is used. H_0 is the single-particle Hamiltonian operator, and Σ^{R}, Σ^{A}, $\Sigma^{<}$, and $\Sigma^{>}$ are the retarded, advanced, lesser, and greater self-energies, respectively.

III. Implementation

This section describes the implementation of the outlined NEGF formalism for the numerical analysis of CNT-FETs. A tight-binding Hamiltonian is used to describe transport phenomena in a $(17, 0)$ zigzag CNT-FET. The self-energy due to electron-photon interactions are studied next.

A. Tight-Binding Hamiltonian

In graphene three σ bonds hybridize in an sp^2 configuration, whereas the other $2p_z$ orbital, which is perpendicular to the graphene layer, forms π covalent bonds. The π energy bands are predominantly determining the solid state properties of graphene. Similar considerations hold for CNTs. We use a nearest-neighbor tight-binding π-bond model [6]. Each atom in an sp^2-coordinated CNT has three nearest neighbors, located $a_{\mathrm{cc}} = 1.42$ Å away. The band-structure consists of π-orbitals only, with the hopping parameter $t = V_{pp\pi} \approx -2.7$ eV and zero on-site potential. By transforming from real space into eigen mode space [6, 11], the subbands become decoupled. Details can be found in [9, 12].

B. Electron-Photon Self-Energies

The Hamiltonian of the electron-photon interaction can be written as [13, 14]:

$$\hat{H}_{e-ph} = \sum_{l,m} M_{l,m} \left(\hat{b} e^{-i\omega t} + \hat{b}^{\dagger} e^{+i\omega t} \right) \hat{a}_l^{\dagger} \hat{a}_m \tag{3}$$

$$M_{l,m} = (z_m - z_l)\, \frac{i\mathrm{e}}{\hbar} \sqrt{\frac{\hbar I_{\omega}}{2N\omega\epsilon c}} \langle l | \hat{H}_0 | m \rangle \tag{4}$$

where z_m denotes the position of the carbon atom at site m, I_{ω} is the flux of photons with the frequency ω, and N is the photon number in the control volume. The incident light is assumed to be monochromatic, with polarization along the CNT axis, see Fig. 1.

We employed the lowest order self-energy of the electron-photon interaction [15]:

$$\begin{aligned} \Sigma^{<,\nu}_{l,m}(E) &= \textstyle\sum_{p,q} M_{l,p} M_{q,m} \\ &\times \left[N G^{<,\nu}_{p,q}(E - \hbar\omega) + (N+1) G^{<,\nu}_{p,q}(E + \hbar\omega) \right] \end{aligned} \tag{5}$$

The first term corresponds to the excitation of an electron by the absorption of a photon and the second term corresponds to the emission of a photon by de-excitation of an electron. The greater self-energy is calculated analogously and the retarded self-energy can be approximated as $\Sigma^{\mathrm{R}} = [\Sigma^{>} - \Sigma^{<}]/2i$. The transport equations must be iterated to achieve convergence of the electron-photon self-energies, resulting in a self-consistent Born approximation.

978-1-4244-2307-1/08/$25.00 ©2008 IEEE

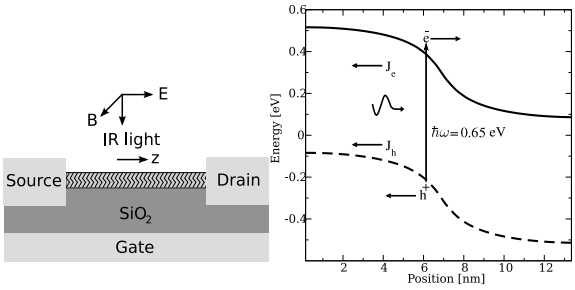

Fig. 1. a) The sketch of a CNT-FET with $L_{\mathrm{CNT}} = 13$ nm. b) The process of electron-hole generation by photo-absorption. Incident photons generate electron-hole pairs and the electric field drives electrons and holes towards the drain and source contacts, respectively. $E_{\mathrm{G}} = 0.6$ eV, $\hbar\omega = 0.65$ eV, and $E_{\mathrm{fs}} = V_{\mathrm{fd}} = 0.0$ V. For the given photon energy the first subband contributes mostly to the total photo-current.

IV. Results

Under steady-state condition the Green's functions $G(r_1, r_2; E)$ in the coordinate representation depend on two positions arguments r_1, r_2 and one energy argument E. For a numerical solution, each argument of the Green's function needs to be discretized. A couple of hundred grid points for each argument results in an overall large memory requirement. When scattering via a self-energy is introduced, the determination of the Green's function requires inversion of a matrix of huge rank. To reduce the computational cost, the *local scattering approximation* is frequently used [6–8, 15–17]. In this approximation the scattering self-energy terms are diagonal in coordinate representation. It allows one to employ the recursive algorithm for computing the Green's functions [15, 18]. The local approximation is well justified for electron-phonon scattering caused by deformation potential interaction [8]. However, we show that this approximation is not justified for electron-photon interaction.

For the given structure (Fig. 1) the calculated photo current is shown in Fig. 2. The results are indicated as a function of the number of included off-diagonal elements of the retarded self-energy, which includes the effects of electron-photon interaction. By including only the diagonal elements of the self-energy (local scattering approximation) the calculated current is only four percent of its value in case of full matrix consideration. This behavior can be well understood by

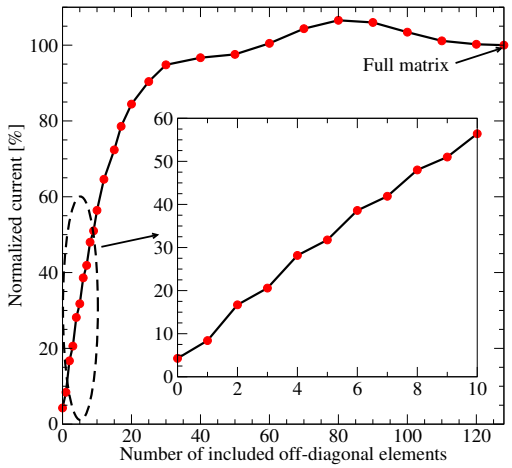

Fig. 2. The calculated photo-current as a function of the included off-diagonal elements of the retarded self-energy (Σ^{R}). The current is normalized to the value with full matrix elements. The full matrix size is 128×128.

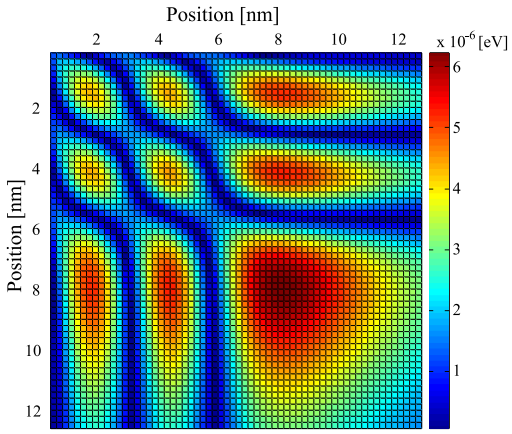

Fig. 3. The retarded self-energy (Σ^{R}) in coordinate representation for $E = 1.55$ eV. The existence of relatively strong off-diagonal elements indicate the non-locality of the interaction and the need to include the full matrix.

considering the self-energy in two coordinate representation. As shown in Fig. 3 off-diagonal elements are relatively strong which indicate the need for a full matrix description.

The oscillations in the self-energy result from the wave-like behavior in the quasi ballistic regime. This phenomenon is also present in Fig. 2. By increasing the number of included off-diagonal elements to around 50, the calculated photo-current increases. However, from this point the photo-current oscillates until it reaches its exact value at 128 off-diagonals. At some points the photo-current is even overestimated. It should be noted that change of the sign of the self-energy at some points results in overestimating of the photo-current if the full matrix description is not employed.

V. Conclusion

We present a numerical study of CNT-based photo-detectors employing the NEGF method. The results show that the local scattering approximation, which is widely used in quantum transport simulations, fails to predict the behavior of devices where electron-photon interaction is present. For accurate simulations a non-local self-energy must be taken into consideration.

VI. Acknowledgements

This work, as part of the European Science Foundation EUROCORES Programme FoNE, was partly supported by funds from FWF (Contract I79-N16), CNR, EPSRC, the EC Sixth Framework Programme, under Contract No. ERAS-CT-2003-980409, and by FWF, Contract No. F2509.

References

[1] J. Appenzeller, Proc. IEEE **96**, 201 (2008).
[2] M. Freitag *et al.*, Phys. Rev. Lett. **93**, 076803 (2004).
[3] M. Freitag *et al.*, Nano Lett. **3**, 1067 (2003).
[4] S. Lu *et al.*, Nanotechnology **17**, 1843 (2006).
[5] J. Zhang *et al.*, Proc. SPIE **6395**, 63950A (2006).
[6] A. Svizhenko *et al.*, Phys. Rev. B **72**, 085430 (2005).
[7] J. Guo, J. Appl. Phys. **98**, 063519 (2005).
[8] S. O. Koswatta *et al.*, IEEE Trans. Electron Devices **54**, 2339 (2007).
[9] M. Pourfath *et al.*, Nanotechnology **18**, 424036 (2007).
[10] S. Datta, Superlattices Microstruct. **28**, 253 (2000).
[11] R. Venugopal *et al.*, J. Appl. Phys. **92**, 3730 (2002).
[12] M. Pourfath *et al.*, IOP J. Phys.: Conf. Ser. **38**, 29 (2006).
[13] E. Lindor *et al.*, J. Appl. Phys. **91**, 6273 (2002).
[14] D. A. Stewart *et al.*, Phys. Rev. Lett. **93**, 107401 (2004).
[15] R. Lake *et al.*, J. Appl. Phys. **81**, 7845 (1997).
[16] S. Datta, J. Phys.:Condensed Matter **2**, 8023 (1990).
[17] R. Lake *et al.*, Phys. Rev. B **45**, 6670 (1992).
[18] A. Svizhenko *et al.*, J. Appl. Phys. **91**, 2343 (2002).